Title	Graphene biosensor programming with genetically engineered fusion protein monolayers
Author(s)	Soikkeli, Miika; Kurppa, Katri; Kainlauri, Markku; Arpiainen, Sanna; Paananen, Arja; Gunnarsson, David; Joensuu, Jussi J.; Laaksonen, Päivi; Prunnila, Mika; Linder, Markus B.; Ahopelto, Jouni
Citation	ACS Applied Materials and Interfaces. American Chemical Society . Vol. 8 (2016) No: 12, Pages 8257-8264
Date	2016
Rights	This is a accepted manuscript of the article and it may be downloaded for personal use use only.

Graphene biosensor programming with genetically engineered fusion protein monolayers

Miika Soikkeli[‡1], Katri Kurppa[‡1], Markku Kainlauri[‡1], Sanna Arpiainen[‡1], Arja Paananen[1],

David Gunnarsson[1], Jussi J. Joensuu[1], Päivi Laaksonen[1†], Mika Prunnila[1],

Markus B. Linder[1,2], Jouni Ahopelto[‡1]*

[1]VTT Technical Research Centre of Finland Ltd, P.O. Box 1000, FI-02044 VTT, Espoo, Finland

[2] Aalto University, School of Chemical Technology, P.O. Box 6100, FI-00076 AALTO, Espoo, Finland

†Present Address: Aalto University, School of Chemical Technology, P.O. Box 16200, FI-00076 AALTO, Finland

KEYWORDS graphene, biosensor, fusion protein, hydrophobin, self-assembly, Debye length

ABSTRACT We demonstrate a label-free biosensor concept based on specific receptor modules providing immobilization and selectivity to the desired analyte molecules, and on charge sensing with a graphene field effect transistor. The receptor modules are fusion proteins in which small hydrophobin proteins act as the anchor to immobilize the receptor moiety. The functionalization of the graphene sensor is a single step process based on directed self-assembly of the receptor modules on a hydrophobic surface. The modules are produced separately in fungi or plants and purified before use. The modules form a dense and well-oriented monolayer on the graphene transistor channel and the receptor module monolayer can be removed and a new module monolayer with a different selectivity can be assembled in situ. The receptor module monolayers survive drying, showing that the functionalized devices can be stored and have a reasonable shelf-life. The sensor is tested with small charged peptides and large immunoglobulin molecules. The measured sensitivities are in the femtomolar range and the response is relatively fast, of the order of one second.

1. Introduction

Health and well-being is recognized as one of the growing challenges in today's ageing society requiring easy-to-use monitoring tools for daily life. One of the emerging trends is preventive health care, which is turning research towards point-of-care diagnostics and qualitative and quantitative detection of biological and chemical species such as disease markers.[1] In many cases culturing and labelling is required, making diagnostics slow and sometimes even cumbersome, directing the efforts to development of label-free techniques. Quantitative label free charge based detection of analytes has been recently demonstrated with carbon nanotube (CNT), graphene and semiconductor nanowire based sensors.[2-5] Regarding graphene, different forms varying from functionalized reduced graphene oxide (rGO) mixtures to pristine graphene have been utilized in sensors.[6-10] Graphene field effect transistors (GFET) are extremely sensitive to charges residing in the vicinity of the graphene channel.[11] Charges have a strong effect on the position of the Dirac peak, which provides a measure of the amount of charge carried by the analytes. Because most biomolecules, such as antibodies, DNA, peptides, proteins and lipids are inherently charged, their detection with field effect sensors is essentially label-free. Compared to other FET-type sensors, for example silicon nanowires, GFETs have similar charge sensitivity but larger surface area for functionalization, higher chemical stability and much larger fabrication tolerances. The main challenges are related to bio-recognition, particularly to the reliable and reproducible immobilization of the receptor layer for selective binding of the desired analyte.

Hydrophobin proteins have been optimized by evolution to assemble at interfaces.[12] The proteins have a hydrophobic patch which binds relatively strongly to hydrophobic surfaces, such as graphene, through van der Waals interactions and form a dense monomolecular layer with a specific molecular orientation,[13-16] Hydrophobin binding on graphene has been previously utilized to exfoliate graphene[15] and to employ hydrophobin fusion proteins as binders in graphene-nanofibrillous cellulose composites[17]. Hydrophobins have also been used with immobilized glucose oxidase in amperometric sensing of glucose on platinum,[18] in multi-wall carbon nanotube electrodes[19] and with immobilized choline oxidase for choline detection on gold electrodes.[20]

In this work, we report on a generic biosensor concept which combines the high charge sensitivity of the GFET with receptor modules that are produced separately providing both the immobilization and sensing functions. Receptor modules are fusion proteins with the receptor molecule genetically attached to an HFBI hydrophobin anchor which provides the immobilization. The modules are produced in fungi or plants using fusion techniques and are purified before use. The attachment relies on directed self-assembly, resulting in a dense and well-oriented monolayer of the modules on the GFET channel. The approach enables a single step in situ functionalization of the sensor with purified receptor modules, and also in situ removal of the modules and re-functionalization, i.e., programming. In addition, it is shown that the module monolayers on GFET survive drying and re-wetting without losing sensitivity to analyte, thus making possible to realize disposable chips which are sensitized to a preselected analyte. We first demonstrate the sensor concept using receptor modules with HFBI anchor and Z_E peptide as the receptor to detect the Z_R peptide. The advantage of these helical peptides is their small size which should not hinder the self-assembly of the hydrophobins on graphene, and their relatively well defined charge. As a more realistic test case we use HFBI-Protein A receptor modules and immunoglobulin analyte. Protein A is known to bind different immunoglobulin subclasses, with highest affinity to the members of the IgG class and was applied here to detect IgG1 antibody. The sensor device and measurement configuration are schematically depicted in Figure 1.

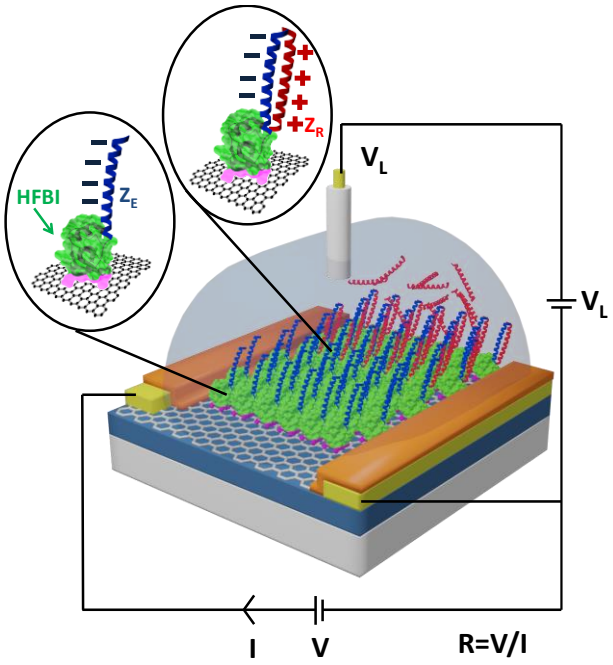

Figure 1. Functionalized GFET biosensor and measurement configuration shown schematically. V_L is the liquid gate voltage and R is the graphene channel resistance. In this case the GFET channel is functionalized with a monolayer of HFBI-Z_E receptor modules and the charge of the modules define the resistance of the channel, i.e., fix the position of the Dirac peak. The analyte molecules bound by the receptors shift the position of the peak and the amount of the shift provides information of the concentration of the analyte in the sample.

2. Experimental section

Fabrication of the graphene field effect transistors. GFETs were fabricated from graphene grown by photo-thermal chemical vapour deposition (PT-CVD) on copper foil (Alfa Aesar, 99.999 %).[21] Monolayer graphene was transferred using a sacrificial polymethylmethacrylate (PMMA) support onto a silicon substrate covered with a 300 nm thick thermal silicon dioxide layer. The SiO_2 surface was treated with hexamethyldisilazane (HMDS) to promote adhesion and to enhance the electrical characteristics of graphene.[22] The copper foil was etched in alkaline solution. PMMA support was removed in subsequent ultrasonic baths of acetone, isopropanol and de-ionized water, followed by a 3 hour anneal at 350 °C in vacuum. The clean graphene surface was protected with a 20 nm thick TiO_2 layer grown by atomic layer deposition (ALD). To initiate the ALD growth, a 1 nm thick layer of Ti was first evaporated on graphene and was allowed to oxidize. Graphene was patterned using optical lithography and oxygen plasma. The electrical contacts were formed by thin evaporated Ti/Au (5/50 nm) metallization and lift-off. The electrodes around the channels were protected from the liquid environment with a 85 nm thick TiO_2 layer grown by ALD. 30 µm x 190 µm graphene channels were opened in polysilicon etch and the chips were wire bonded to chip carriers.

Receptor modules and analytes. HFBI-Protein A modules were produced in transient expression mode in *Nicotiana tabacum* plants via agroinfiltration as described previously.[23] Proteins were extracted for purification by homogenizing frozen leaves in PBS buffer supplemented with 2% (W/V) sodium ascorbate, and 1 mM EDTA (4x buffer volume/leaf weight). The homogenate was clarified twice by centrifugation (10 min at 3220 g at 4 ^{o}C). The supernatant was warmed to RT and mixed with Triton X-114 (3% w/v, Sigma Aldrich, USA). The phases were allowed to separate at room temperature. The top (detergent-poor) phase was removed and the detergent phase was washed with isobutanol (10x volume / detergent mass). After

buffer exchange, the extract was polished by affinity chromatography using a Streptactin macroprep column according the manufacturers protocol (IBA, Germany).

The fusion protein HFBI-Z_E was produced in the filamentous fungus *Trichoderma reesei*.[15] The fusion proteins were purified by standard two-phase extraction procedure as described previously.[23, 24] Proteins were diluted to the concentration of 0.1 mg/ml in the buffer solution (100 mM sodium phosphate pH 7). This concentration has been found to suit best to QCM investigations with hydrophobin fusions.

Sequences of Z_E and Z_R regions [25]

Z_E: L E I E A A F L E Q E N T A L E T E V A E L E Q E V Q R L E N I V S Q Y R T R Y P G L

Z_R: L E I R A A F L R R R N T A L R T R V A E L R Q R V Q R L R N E V S Q Y E T R Y G P L

The analyte for HFBI-Z_E was a synthetic peptide Z_R (5 kDa, Biomatik Co., Ontario, Canada) and for HFBI-Protein A antibody IgG1 lambda (150 kDa, Sigma Aldrich, St.Louis, USA).

The estimation of net charges of the peptides and hydrophobin was carried out by summing the charges of each of the amino acids using the pKa values. For Z_E and Z_R the assumption was that all the side chains can have effect on the net charge. For HFBI the cysteine amino acids were excluded from the net charge calculation since it is known that they form sulfur bridges with each other thus stabilizing the hydrophobin structure, and not affecting the net charge. [26]

Atomic force microscopy (AFM). Topography images of HFBI – Protein A and HFBI – Z_E layers on graphene were captured with NanoScopeV Multimode8 AFM (E scanner, Bruker). As deposited CVD graphene on catalytic metal surface (Pt) and CVD graphene transferred on SiO_2 were used as substrates. Self-assembly of the receptor module layers was performed in identical conditions that were used for GFET sensor programming. Freshly prepared module layers were imaged first in the buffer solution (100 mM NaP, pH 7) in ScanAsyst mode using ScanAsyst-Fluid+ cantilevers for SiO_2 samples (the images are shown in SI) and Fluid cantilevers for Pt samples (Bruker, f_0 = 150 kHz, k = 0.7 N/m) with a scan rate of 1.6 Hz. After imaging in buffer, the module layers were rinsed gently with buffer and milli-Q water and dried under N_2. Samples were stored in a container under N_2 for 1 to 3 hours before imaging in dry state. Images of dry module layers were recorded in the ScanAsyst mode in air using ScanAsyst-Air cantilevers (Bruker, f_0 = 70 kHz, k = 0.4 N/m) with a scan rate of 1.6 Hz. These conditions were used also for the clean graphene surfaces. Re-wetting of module layers was carried out by placing buffer solution on the sample surface and starting imaging in buffer within 5 to 15 min. Imaging was performed as described above for the freshly prepared samples. Images were flattened to remove possible tilt in the image data, and no further image processing was performed. The NanoScope Analysis software (Bruker) was used for image processing and analysis.

Quartz crystal microbalance (QCM-D) measurements. A QCM-D (E4, Biolin Scientific, Sweden) was used to measure the binding of HFBI - Protein A and HFBI-Z_E modules on hydrophobic substrates, and the binding of the corresponding analytes to the receptor modules. Polystyrene coated 5 MHz quartz crystals were purchased ready-made at Biolin Scientific or spin-coated on gold coated crystals according to supplier's protocol. Binding on graphene was tested with CVD graphene transferred on the crystals. The crystals were rinsed with ethanol and MQ water and dried with N_2 prior to measurement. Buffer solution was 100 mM sodium phosphate at pH 7. In analysis, solution of HFBI-Z_E or HFBI-Protein A diluted in the buffer (100 µg/ml, 500 µl) was pumped into the measurement chamber at 0.1 ml/min rate. The adsorbed layer was

next rinsed with the buffer. Treatment was repeated, but additional binding was not detected. The analyte solution was then injected into the chamber and rinsed with the buffer to monitor selective binding.

Electrical measurements and fluidic set-up. All the measurements were performed using a single GFET. The sensor was analyzed using a fluidic chamber formed by mechanically clamping a cover to the sensor chip with an O-ring sealing. The polyether ether ketone (PEEK) cover had tubing for liquid inlet and outlet and for a Ag/AgCl reference electrode (1 mm diameter leak free reference electrode by Harvard Apparatus). The functionalization of the graphene channel was carried out using a similar cover without the electrode. A computer controlled syringe pump system was used to feed controlled amounts of protein and buffer solutions into the chamber. The liquid gate potential was controlled by applying a voltage to the Ag/AgCl reference electrode by a semiconductor parameter analyzer (HP4142B). The resistance of the graphene channel was measured in 4-point configuration using a lock-in amplifier with 100 nA AC-bias at a frequency of 11.433 Hz. The silicon substrate of the graphene sensor chip was grounded. The data has not been normalized.

Sensor analysis. Before each series of measurements the graphene surface was cleaned with 3 ml of acetone and ethanol and 10 ml of DI water. Then 3 ml of the buffer was introduced and the resistance of the graphene channel was recorded as a function of liquid potential after 25 min stabilization. The sensor was functionalized by flushing with HFBI-Z_E or HFBI-Protein A solution (100 µg/ml) for 3 min at 0.3 ml/min flux. The surface was let to stabilize for 60 min, rinsed with the buffer solution for 5 min and dried with N_2. The fluidic chamber was replaced by a clean one and the sensor was rinsed again with the buffer and the channel resistance was measured. Sensitivity measurements were performed with the analytes described in the Receptor modules and analytes section above, with 1 min pumping and 25 min stabilization for each concentration. To test the effect of the buffer concentration on the sensitivity, the clean sensor was first measured in 10 mM and 100 mM NaP buffers. Then the sensor was functionalized with HFBI-Z_E receptor modules as described above and measured in the 10 mM buffer and subsequently in the 100 mM buffer solution.

3. Results and discussion

Directed self-assembly and surface coverage. High surface coverage and packing density of the receptor modules are essential to obtain high sensitivity via optimal net affinity of the specific analyte and to prevent unspecific binding from the analyte medium. It has been shown earlier that HFBI proteins form a full dense monolayer on highly ordered pyrolytic graphite.[16] In this work we have investigated the surface coverage of the HFBI-Z_E and HFBI-Protein A receptor modules formed by a single step directed self-assembly. The surface coverage was studied using AFM both in liquid and dry conditions. AFM images of a clean CVD graphene surface on platinum as well as both HFBI-Z_E and HFBI-Protein A functionalized surfaces are shown in Figure 2. The surfaces were imaged in wet state in sodium phosphate buffer immediately after the functionalization, after drying for a few hours in N_2 and finally after re-wetting in the buffer. Both receptor modules form a dense surface monolayer layer immediately after the functionalization. Drying can induce some cracks in the layer but after re-wetting in the buffer solution the module monolayer is healed and no cracks can be observed. The thicknesses of both dried HFBI- Z_E and HFBI-Protein A layers are within 4 to 5 nm, which fits well to the thickness of a monomolecular layer of hydrophobins in the dry state.[27] The results are similar on graphene transferred onto SiO_2 and the corresponding AFM images can be found in the SI.

Quartz crystal microbalance measurements. The AFM results are further confirmed by the QCM analysis showing that the self-assembly of the HFBI-Z_E modules on a hydrophobic polystyrene surface creates a rigid monolayer with surface coverage close to unity (see SI). The QCM data of self-assembly of HFBI-Protein A

receptor modules on hydrophobic polystyrene surface and the subsequent response to introduction of IgG1 analyte are shown in Figure 3.

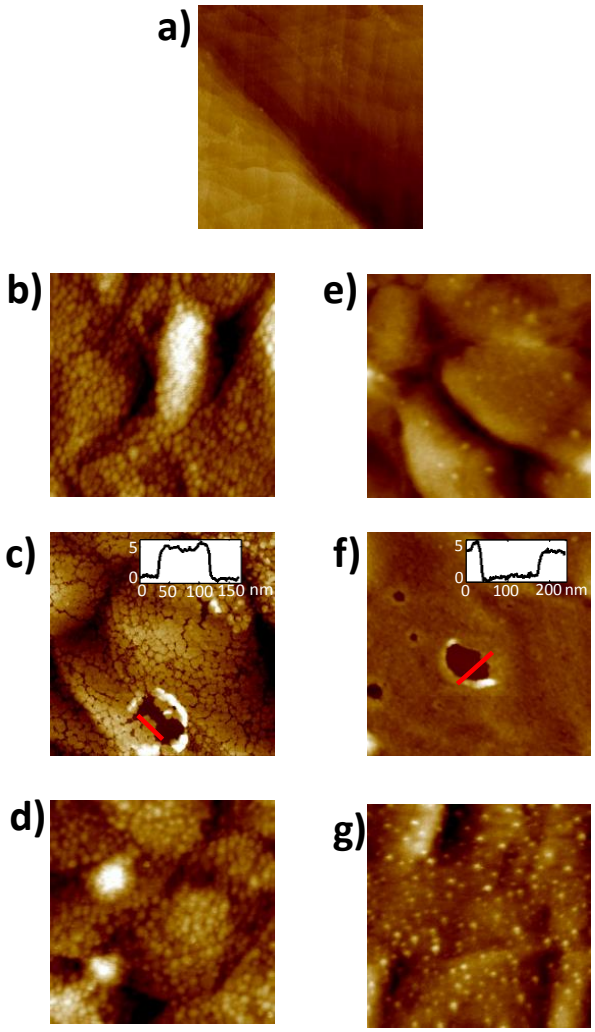

Figure 2. Atomic force microscopy topography images of clean, HFBI-Z_E and HFBI-Protein A receptor module layers on CVD graphene on platinum. a) Clean graphene surface on platinum before any functionalization. b) Surface after HFBI-Z_E functionalization in 100 mM pH 7 NaP buffer, c) after drying in N2 and d) after re-wetting in the buffer. e) Surface after HFBI-Protein A functionalization in 100 mM pH 7 NaP buffer, f) after drying and g) after re-wetting in the buffer. For both of the receptor modules protein film shrinkage and possible mechanical forces during the drying tend to create cracks in the film but damage is healed in both cases after 5 min re-wetting in the buffer. The height profiles of the dried samples in the insets of figures c) and f) correspond to the red lines in the same figures. The thickness of both the dried HFBI-Z_E and HFBI-Protein A layers is 4 to 5 nm, corresponding to a typical thickness of a monomolecular fusion protein layer after drying. The image size is 1 x 1 μm^2 and height scale 15 nm in all the images.

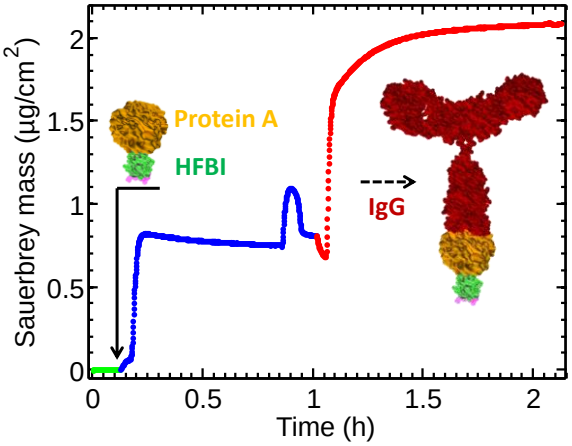

Figure 3. QCM sensogram showing the formation of the HFBI-Protein A receptor module layer on hydrophobic polystyrene surface together with the subsequent binding of the IgG1 analyte. The blue curve shows the mass increase due to the self-assembly of the monolayer of the receptor modules and the red the subsequent binding of the analyte. The introduction of the receptor modules and the analyte are indicated by arrows. The hump at the end of the blue curve is due to a rinse pulse with the buffer.

The Sauerbrey mass of the HFBI-Protein A monolayer corresponds to an average 3.2±0.2 nm spacing between the molecules (see SI). This agrees with the estimated diameter of the Protein A part of the HFBI-Protein A fusion,[28] suggesting formation of a uniform and dense surface coverage, agreeing with the AFM results. From the QCM data the IgG1 binding ratio to the receptor modules was found to be roughly 50 – 60 % at 8 nM analyte concentration (see SI for details). The HFBI-Protein A module binding on different hydrophobic surfaces such as polystyrene (Figure 3) and CVD graphene transferred to the quartz crystal gave similar results, verifying the hydrophobicity-mediated adhesion (see SI).

Sensor response. Charged zipper peptide pair Z_E-Z_R was used to demonstrate the operation principle of the sensor. These peptides are well suited to test the operation and sensitivity due to their same but opposite charges and small size without hindering the formation of a uniform module monolayer on graphene, as shown in Figure 2. The estimation of the charge states of HFBI protein and Z_E and Z_R peptides as a function of pH are shown in Figure 4a. HFBI has a nearly neutral net charge around pH 7 and the total charge of Z_E and Z_R are -7e and +7e, respectively. Consequently, the net charge of HFBI-Z_E receptor module is expected to be -7 which will be compensated by the charge of the Z_R analyte during binding by ionic bridging between the matching amino acids[25]. The Z_R concentration of 10 µM is expected to provide an ideal 1:1 binding ratio with Z_E (see SI).

The response of the sensor was measured with only buffer solution introduced, after in situ self-assembly of a HFBI-Z_E module layer and after binding of the Z_R analyte. After functionalization with HFBI-Z_E receptor modules, the sensor was dried and the fluidic chamber was replaced with a clean one to avoid possible memory effects in the liquid feeding tubing. The shift of the Dirac peak and the corresponding relative change in the channel resistance arising from the functionalization and introduction of the analyte are plotted in Figures 4b and 4c, respectively. All the measurements were carried out in 100 mM sodium phosphate buffer at pH7. The shift of the Dirac peak towards more positive voltage indicates that the HFBI-Z_E complex carries negative charge, (blue curve in Figure 4b) consistent with the calculations shown in Figure 4a. Introduction of the peptide Z_R in 10 µM analyte solution (red curve in Figure 4b) returned the Dirac peak position close to the value of the clean sensor state (green curve in Figure 4b), indicating effectively zero net charge of the peptide pair. The sensitivity was investigated at constant liquid gate voltage V_L by introducing

the Z_R analyte in increasing concentrations as shown in Figure 4d and measuring the channel resistance at constant V_L. The liquid gate bias V_L = 0 V was selected to optimize the response by producing maximum ΔR.

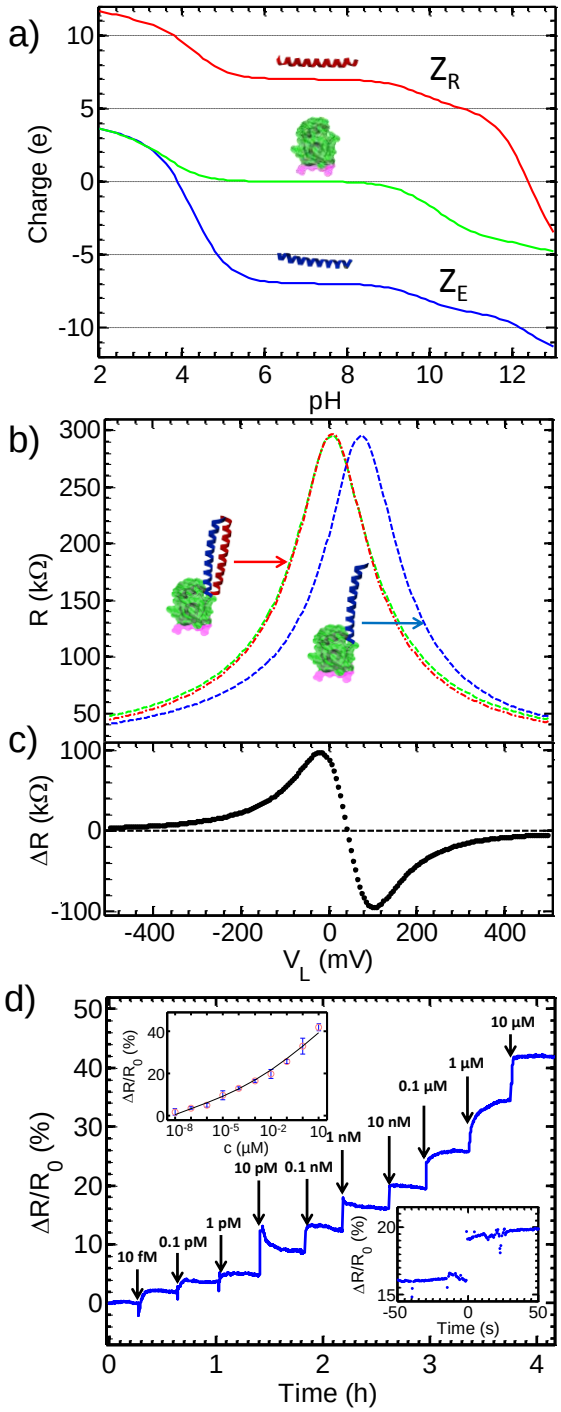

Figure 4. (a) Calculated charge of the peptides Z_E (blue) and Z_R (red), and the hydrophobin protein HFBI (green) as a function of pH. (b) Resistance of the graphene channel as a function of the liquid potential for clean graphene surface (green), with HFBI-Z_E receptor module surface functionalization (blue) and after selective binding of Z_R from 10 μM analyte solution (red). (c) Resistance difference ΔR arising from the Z_R binding, i.e., subtraction of the blue curve from the red curve. (d) Sensor response at increasing Z_R analyte concentration. The arrows indicate the introduction of the analyte and the concentrations. The calibration curve defined as the average response measured at each concentration level (error bars 2σ) is shown in the top inset. Initial and end states in (d) correspond to the blue and red curves in (b). (bottom inset) Close-up of the the response curve showing the abrupt rise of the signal as for 10 nM step.

The dynamic range of detection was found to extend from 10 fM at least up to 10 µM analyte concentration. Already 10 fM analyte concentration induced a saturated response of 2 % in the relative change of the channel resistance at constant V_L, an order of magnitude higher than the noise level in the measurement. The detector response was fast, typically less than 1 s, reflecting the immediate receptor-analyte binding process (see the bottom inset in Figure 4d). After the initial response, the stabilization to the biological equilibrium can be affected by curls in the fluidic chamber and mobile charges in the sensor substrate. At very low analyte concentration the association rate is strongly limited by the finite mass transport in the buffer.[29]

The response of HFBI-Protein A receptor module functionalization to IgG1 analyte was investigated in the same way as with the HFBI-Z_E module and Z_R analyte. The response was measured using the same GFET device after in situ solvent cleaning followed by functionalization with the new receptor modules. Again, the modules form a full monolayer on graphene by self-assembling, as shown in Figures 2e, 2f, and 2g. Binding of the HFBI-Protein A receptor module was found to induce a negative shift of the Dirac peak, and the subsequent IgG1 binding further increased the shift, indicating detection of positive charge in both cases. The exact charge of IgG1 is not known. The shift of the Dirac peak and the corresponding change in resistance are shown in Figures 5a and 5b. The sensor sensitivity and the related calibration curve at liquid potential V_L = 75 mV are shown in Figure 5c. A response of about 3 % in the relative change of the channel resistance was obtained at the lowest concentration of 80 fM and the dynamic range was found to extend at least up to 80 nM concentration which was the highest concentration tested. The temporal response of HFBI-Protein A to IgG1was similar to the HFBI-Z_E Z_R system, i.e., fast initial response and slower saturation.

The selectivity of the sensor was studied by functionalizing the graphene surface with HFBI – Z_E receptor modules and using 80 nM IgG1 analyte. IgG1 analyte showed less than 1 % response compared to the 42 % response in $\Delta R/R$ with 10 µM Z_R analyte. In addition, the selectivity was tested using clean graphene channel with no functionalization and also with HFBI anchor protein monolayer functionalization. The response was measured with 10 µM Z_R analyte. Both of the non-functionalized and GFET functionalized only with HFBI proteins gave an order of magnitude smaller shift of the Dirac peak than the sensor with HFBI – Z_E module functionalized surface. Data for selectivity measurements is shown in SI.

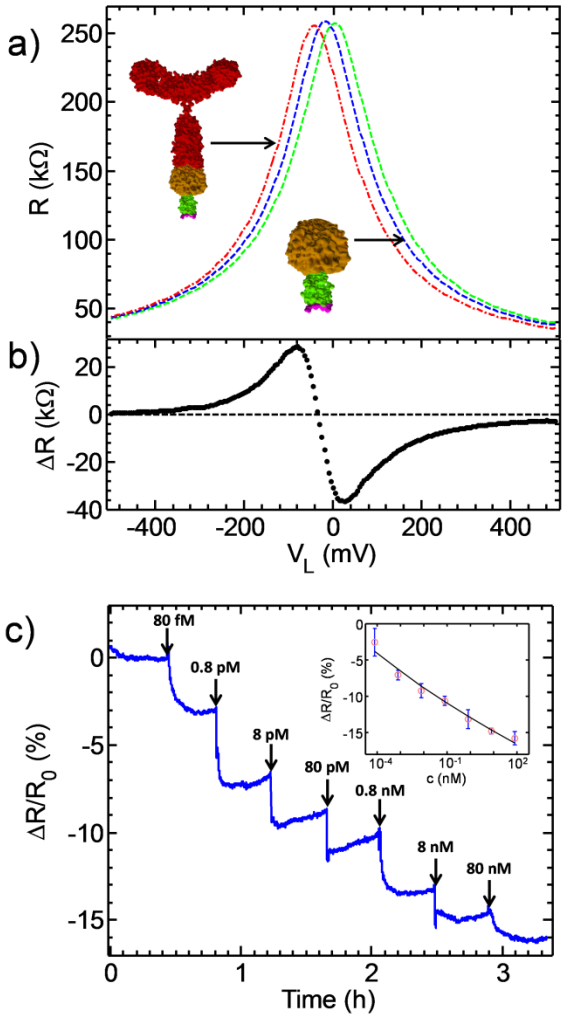

Figure 5. Sensor response to IgG1 with HFBI-Protein A as the receptor module (a) Resistance of the graphene channel as a function of the liquid gate potential for a clean sensor (green), surface functionalized with HFBI-Protein A receptor modules (blue) and after binding of IgG1 from 80 nM analyte solution (red). (b) Resistance difference ΔR arising from the IgG1 binding. (c) Sensor response at increasing IgG1 concentrations and the calibration curve (inset). The arrows indicate the introduction of the analyte and the concentrations. Initial and end states correspond to the blue and red curves in (a).

The measured sensitivity is rather surprising taking into account that the measurements were performed in high ionic strength buffer. The polarizability of the buffer liquid leads to screening of the charge of the analytes, which will limit the sensitivity of the GFET, and consequently, the structure of the immobilized layer has an important role in optimizing the performance of the sensor.[30] Hydrophobins are 3 nm tall[13] and they self-assemble into a dense molecular monolayer on hydrophobic surfaces (see Figure 2). The liquid content remaining inside these layers has been estimated to be only in the range of 10 – 30 %.[31] It is not precisely known how the ionic screening occurs in such a system. The confinement and the small amount of liquid in the protein layer most likely reduces the overall polarizability.[32] Therefore it can be expected that the double layer formation by mobile ions in the liquid takes place mainly above and in between the proteins of the receptor modules, with some contribution arising from the volume of mobile liquid inside the proteins. The effective detection range and the charge sensitivity were investigated with the HFBI-Z_E receptor module monolayer at low analyte concentrations and in two different buffer strengths. The Z_E peptide is linked to the N-terminus of HFBI, which is located in the upper half of the HFBI as illustrated in Figure 6. Each of the Z_E

charges, distributed evenly along the 5 – 6 nm alpha helix,[33] has a different effect on the resistance of the graphene channel due to the different distance and different screening. The sensitivity to the Z_E charges at 100 mM buffer indicates the effective detection range to be of at least 2.5 nm. When the Debye length in the buffer was tripled to 2.1 nm by decreasing the ionic strength of the buffer to 10 mM, the sensor response increased 6 % due to a 25 % (6 mV) larger shift of the Dirac peak (see SI for the data), showing that screening plays a role but the effect is not directly proportional to the Debye length in the bulk of the buffer. Due to the sensitivity to the Debye length, it is expected that the there are certain limitations in the applicability of the sensor at very high ionic strengths. However, a measurable signal for selective detection at conditions close to physiological conditions was obtained.

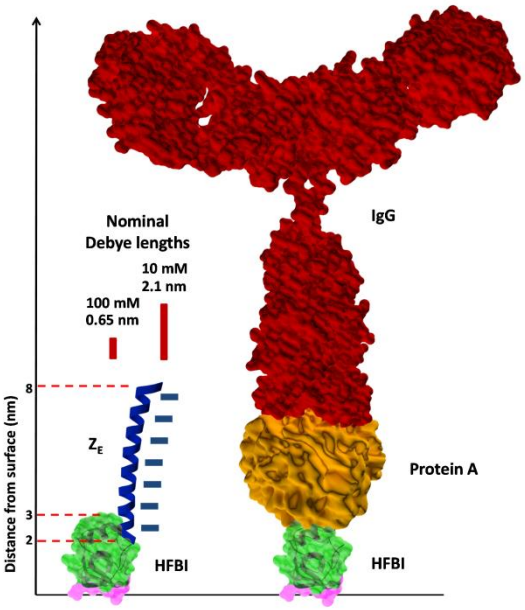

Figure 6. Illustration of the sizes and the relevant length scales related to the response of the sensor. The nominal Debye lengths in 10 mM and 100 mM buffer solutions are shown by red bars. The effective detection distance from the graphene surface found in the measurements is much larger than the bulk solution Debye lengths.

The case of HFBI-Protein A receptor module and IgG1 analyte is more problematic. Protein A is larger molecule than HFBI and steric hindrance during self-assembly can affect the formation of the receptor layer on the graphene channel. However, as shown by the AFM images in the Figure 2 and by the QCM results, the HFBI-Protein A receptor modules form a dense monolayer and the reasoning of reduced screening should apply also here, extending the detection range of the charge carried by the large biomolecules. The size of the fusion receptors suggests the distance of the binding site of IgG1 to be at least 5 nm from the graphene surface, which is in accordance with layer thicknesses estimated from QCM and the AFM data. This is again significantly larger than the sub-nanometer Debye length in the buffer solution. The IgG1 molecules are large (~15 nm) and the sensor is expected to detect only part of the charges of the molecule. The net charge of the IgG1 molecules at pH 7 is positive (pI 8 – 9.5), which is consistent with the measured response. The amount and location of the charge within the IgG1 molecule is not known and the orientation of the molecule can depend on the binding ratio to Protein A. At low analyte concentrations the IgG1 molecules have enough space to lie down on top of the Protein A layer, but at high binding ratios these molecules are probably standing perpendicular to the surface due to the Coulomb repulsion forces. The limited volume of liquid inside the dense IgG1 molecule layer might enhance the effective detection range at high analyte concentrations. However, the experimental data shows that the GFET functionalized with the

receptor module monolayer has high sensitivity even for large molecules in strong ionic buffer, is label-free and selective. The conditions chosen for the study simulate the blood plasma, showing the applicability of the technology for blood analytics. At neutral pH, the hydrophobin layer has neutral or slightly negative charge which repels negatively charged albumins and fibrinogen and therefore suits perfectly for a passive layer for supporting the actual sensing motifs.The sensing group itself is specific for binding of the analyte, which limits the risks of false positive responses.

4. Conclusions

In this work we have demonstrated the concept of a modular and programmable label-free biosensor. The receptor modules, consisting of an anchor for immobilization and receptor for recognition, are separately produced by biological fusion and pre-purified before use. The receptor moiety can be selected to match the analyte to be detected, and the anchoring moiety is always the HFBI hydrophobin protein. It is shown that the receptor modules form a dense oriented monomolecular layer by a single step directed self-assembly on the graphene channel of the GFET used for charge detection. Because most of the biological molecules carry charge, specific labelling is not required. The GFET provides very high charge sensitivity and is fabricated by rather standard microelectronics processing techniques, facilitating mass production of the sensors. The sensitivity of the biorecognition in both model systems is high, with 3 % response recorded for below 100 fM analyte concentrations in high ionic strength buffer. The potential to build in selectivity is demonstrated by cross-checking with immunoglobulin analyte and a sensor functionalized with receptor modules for peptide analyte, resulting an order of magnitude smaller shift in the position of the Dirac peak and, consequently much smaller $\Delta R/R$ response with the IgG1 analyte compared to the peptide analyte. However, several challenges remain to be solved when working with real samples due to their complexity. It is shown that the same device can be programmed to detect different analytes by changing the receptor module layer in situ. The possibility to dry the receptor module layer on the sensor without compromising the performance will be essential for pre-programmed sensor assays in point-of-care applications exploiting disposable sensor chips.

ASSOCIATED CONTENT

Supporting Information

Additional information about SPR and QCM-D analysis, AFM images, calculation of theoretical Debye length and measurements with different buffer concentrations. “This material is available free of charge via the Internet at http://pubs.acs.org.”

AUTHOR INFORMATION

Corresponding Author

* E-mail: jouni.ahopelto@vtt.fi

Author Contributions

‡These authors contributed equally to this work

ACKNOWLEDGMENT

This research was supported by TEKES GraNBis, Academy of Finland Centre of Excellence in Atomic Layer Deposition and grant 250898 and the EU FP7 Graphene Flagship Project grant n°604391. Ingmar Stuns and Sampo Sorvisto are acknowledged for the fluidic cell. We thank Riitta Suihkonen, Anne Ala-Pöntiö and Teresa Blomqvist for help with production and purification of HFBI – Z_E.

REFERENCES

(1) Ngoepe, M.; Choonara, Y.; Tyagi, C.; Tomar, L.; Toit, L.; Ku-mar, P.; Ndesendo, M.; Pillay, V. Integration of Biosensors and Drug Delivery Technologies for Early Detection and Chronic Management of Illness. *Sensors* **2013**, 13, 7680-7713.

(2) Stine, R.; Mulvaney, S. P.; Robinson, J. T.; Tamanaha, C.R.; Sheehan P. E. Fabrication, Optimization and Use of Graphene Field Effect Sensors. *Anal. Chem*. **2013**, 85, 509-521.

(3) Pumera, M. Graphene in Biosensing. *Mater. Today* **2011**, 14 , 308-315.

(4) Jacobs, C. B.; Peairs, M. J.; Venton, B.J. Review: Carbon Nano-tube Based Electrochemical Sensors for Biomolecules. *Anal. Chim. Acta* **2010**, 662, 105-127.

(5) Chen, K.; Li, B.; Chen, Y. Silicon Nanowire Field-effect Transistor-based Biosensors for Biomedical Diagnosis and Cellular Recording Investigation. *Nano Today* **2011**, 6, 131-154.

(6) Kuila, T.; Bose, S.; Khanra, P.; Mishra, A. K.; Kim, N. H.; Lee, J. H. Recent Advances in Graphene-based Biosensors. *Biosens. Bioelectron*. **2011**, 26, 4637-4648.

(7) Ohno, Y.; Maehashi, K.; Matsumoto, K. Label-free Biosensors Based on Aptamer-modified Graphene Field-effect Transistors. *J.Am.Chem.Soc*. **2010**, 132, 18012-18013.

(8) Mannoor. M. S.; Tao, H.; Clayton, J. D.; Sungupta, A.; Kaplan, D. L.; Naik, R. N.; Verma, N.; Omenetto, F. G.; McAlpine, M. C. Graphene-based Wireless Bacteria Detection on Tooth Enamel. *Nat. Commun*. **2012**, 3, 763.

(9) Cui, Y.; Kim, S. N.; Jones, S. E.; Wissler, L. L.; Naik, R. R.; McAlpine, M. C. Chemical Functionalization of Graphene Ena-bled by Phage Displayed Peptides. *Nano Lett*. **2010**, 10, 4559-4565.

(10) Borini, S.; White, R.; Wei, D.; Astley, M.; Haque, S.; Spigone, E.; Harris, N.; Kivioja, J.; Ryhänen, T. Ultrafast Graphene Oxide Humidity Sensors. *ACS Nano* **2013**, 7, 11166-11173.

(11) Novoselov, K. S.; Geim, A. K.; Morozov, S. V.; Jiang, D.; Zhang, Y.; Dubonos, S. V.; Grigorieva, I. V.; Firsov, A. A. Electric Field Effect in Atomically Thin Carbon Films. *Science* **2004**, 306, 666-669.

(12) Wessels, J. G. H. Hydrophobins, Unique Fungal Proteins. *Mycologist* **2000**, 14, 153-159.

(13) Linder, M. B.; Szilvay, G. R.; Nakari-Setälä, T.; Penttilä, M. E. Hydrophobins: The Protein-amphiphiles of Filamentous Fungi. *FEMS Microbiol. Rev*. **2005**, 29, 877-896.

(14) Kurppa, K.; Jiang, H.; Szilvay, G. R.; Nasibulin, A. G.; Kaup-pinen, E. I.; Linder, M. B. Controlled Hydrid Nanostructures through Protein-Mediated Noncovalent Functionalization of Carbon Nanotubes. *Angew. Chem., Int. Ed*. **2007**, 116, 6566-6569.

(15) Laaksonen, P.; Kainlauri, M.; Laaksonen, T.; Schepetov, A.; Jiang, H.; Ahopelto, J. Interfacial Engineering by Proteins: Exfoliation and Functionalization of Graphene by Hydrophobins. *Angew. Chem., Int. Ed*. **2010**, 49, 4946-4949.

(16) Kivioja, J.; Kurppa, K.; Kaunlauri, M.; Linder, M. B.; Ahopelto, Electrical Transport through Ordered Self-assembled Protein Monolayer Measured by Constant Force Conductive Atomic Force Microscopy. *J. Appl. Phys. Lett*. **2009**, 94, 183901.

(17) Laaksonen, P.; Walther, A.; Malho, J. M.; Kainlauri, M.; Ilkkala, O.; Linder, M. B. Genetic Engineering of Biomimetic Nanocom-posites: Diblock Proteins, Graphene and Nanofibrillated Cellulose. *Angew. Chem., Int. Ed*. **2011**, 50, 8688-8691.

(18) Zhao, Z.; Qiao, M.; Yin, F.; Shao, B.; Wu, B.; Wang, B.; Wang, X.; Qin, X.; Li, S.; Yu, L.; Chen, Q. Amperometric Glucose Biosensor Based on Self-assembly Hydrophobin with High Efficiency of Enzyme Utilization. *Biosens. Bioelectron*. **2007**, 22, 3021-3027.

(19) Wang, X.; Wang, H.; Huang, Y.; Zhao, Z.; Qin, X.; Wang, Y.; Miao; Z.; Chen, Q.; Qiao, M. Noncovalently Functionalized Multi-wall Carbon Nanotubes in Aqueous Solution Using the Hydrophobin HFBI and Their Electroanalytical Application. *Biosens. Bioelectron*. **2010**, 26, 1104-1108.

(20) Zhao. Z.; Wang, H.; Qin, X.; Wang, X.; Qiao, M.; Anzai, J.; Chen, Q. Self-assembled Film of Hydrophobins on Gold Surfaces and Its Application to Electrochemical Biosensing. *Colloids Surf., B.* **2009**, 71, 102-106.

(21) Riikonen, J.; Kim, W.; Li, C.; Svensk, O.; Arpiainen, S.; Kainlauri, M.; Lipsanen, H. Photo-thermal Chemical Vapour Deposition of Graphene on Copper. *Carbon* **2013**, 62, 43-50.

(22) Lafkioti, M.; Krauss, B.; Lohmann, T.; Zschieschang, U.; Klauk, H.; Klitzing, K.; Smet, J. H. Graphene on a Hydrophobic Substrate: Doping Reduction and Hysteresis Suppression under Ambient Conditions. *Nano Lett*. **2010**, 10, 1149-1153.

(23) Joensuu J.J; Conley A.J; Lienemann M.; Brandle J.E.; Linder M.B.; and Menassa R. Hydrophobin fusions for high-level transient protein expression and purification in Nicotiana benthamiana. *Plant Physiol*. **2010**, 152, 622-633.

(24) Linder, M. B.; Qiao, M.; Laumen, F.; Selber, K.; Hyytiä, T.; Nakari-Setälä, T.; Penttilä, M. E. Efficient Purification of Recombinant Proteins Using Hydrophobins as Tags in Surfactant-based Two-phase Systems. *Biochemistry* **2004**, 43, 11873-11882.

(25) Zhang, K.; Diehl, M. R.; Tirrell, D. A. Artificial Polypeptide Scaffold for Protein Immobilization. *J.Am.Chem.Soc*. **2005**, 127, 10136-10137.

(26) Hakanpää, J.; Szilvay, G. R.; Kaljunen, H.; Maksimainen, M.; Linder, M.B; Rouvinen, J. Two crystal structures of Trichoderma reesei hydrophobin HFBI—the structure of a protein amphiphile with and without detergent interaction. *Protein Sci*. **2006**, 15, 2129-2140.

(27) Szilvay, G. R.; Paananen, A.; Laurikainen, K.; Vuorimaa, E.; Lemmetyinen, H.; Peltonen, J.; Linder, M. B. Self-assembled hydrophobin protein films at the air-water interface: structural analysis and molecular engineering. *Biochemistry* **2007**, 46, 2345-2354.

(28) Gouda, H.; Torigoe, H.; Saito, A.; Sato, M.; Arata, Y.; Shimada, Y. Three-dimensional Solution Structure of the B Domain of Staphylococcal Protein A: Comparisons of the Solution and Crystal Structures. *Biochemistry* **1992**, 31, 9665-9672.

(29) Duan, X.; Li, Y.; Rajan, N. K.; Routenberg, D. A.; Modis, Y. Reed, M. A. Quantification of the Affinities and Kinetics of Pro-tein Interactions Using Silicon Nanowire Biosensors. *Nat. Nanotechnol.* **2012**, 7, 401-407.

(30) Stern, E.; Wagner, R.; Sigworth, F. J.; Breaker, R.; Fahmy, T. M.; Reed, M. A. Importance of the Debye Screening Length on Nanowire Field Effect Transistor Sensors. *Nano Lett*. **2007**, 7, 3405-3409.

(31) Krivosheeva, O.; Dėdinaitė, A.; Linder, M. B.; Tilton, R. D.; Claesson, P. M. Kinetic and Equilibrium Aspects of Adsorption and Desorption of Class II Hydrophobins HFBI and HFBII at Silicon Oxynitride/water and Air/water Interfaces. *Langmuir* **2013**, 29, 2683-2691.

(32) Stigliano, A. F. Breakdown of the Debye Polarization Ansatz at Protein-Water Interfaces. *J. Chem. Phys*. **2013**, 138, 225103.

(33) Berg, J. M.; Tymoczko, J. L.; Stryer, L. Biochemistry, 5th edition (W.H. Freeman and Company, New York, 2002).